Swinburne Research Bank
http://researchbank.swinburne.edu.au

SWIN BUR NE

SWINBURNE UNIVERSITY OF TECHNOLOGY

Low energy exciton states in a nanoscopic semiconducting ring

Hui Hu[a], Guang-Ming Zhang[a,b], Jia-Lin Zhu[a,b], Jia-Jiong Xiong[a]

[a]*Department of Physics, Tsinghua University, Beijing 100084, P. R. China*
[b]*Center for Advanced Study, Tsinghua University, Beijing 100084, P. R. China*
(February 1, 2008)

We consider an effective mass model for an electron-hole pair in a simplified confinement potential, which is applicable to both a nanoscopic self-assembled semiconducting InAs ring and a quantum dot. The linear optical susceptibility, proportional to the absorption intensity of near-infrared transmission, is calculated as a function of the ring radius R_0. Compared with the properties of the quantum dot corresponding to the model with a very small radius R_0, our results are in qualitative agreement with the recent experimental measurements by Pettersson *et al.*
PACS numbers: 73.20.Dx, 71.35.-y, 78.66.Fd

Recent progress in nanoscopic fabrication techniques has made it possible to construct self-assembled semiconducting nano-rings inside a completed field-effect transistor [1–4]. The nanoscopic rings may be considered as the best candidate to display various pure quantum effects, as the nano-rings are in the scattering free and few particles limit. By using two complementary spectroscopic techniques, Lorke and collaborators performed the first spectroscopic measurements on semiconducting InGaAs nano-rings occupied one or two electrons [1–3], and the experimental results have attracted a lot of theoretical interests at the moment [5–10]. However, the spectroscopic data of exciton effects in InGaAs nano-rings have also been obtained [11] and clearly exhibited different excitonic properties from the corresponding quantum dots [12–16]. For these experimental results, so far there has been no theoretical analysis yet.

In this paper, we attempt to describe qualitatively the low-lying states and some spectroscopic properties of the semiconducting nano-ring of InAs. Based on an effective mass model Hamiltonian for an electron-hole pair in a simplified confinement potential, the model Hamiltonian is separated into the motion of center of mass, relative motion of the electron-hole pair, and the mixed part. By varying radius of the ring R_0, both the quantum dots and nano-rings are investigated within the same framework of a theory. In the subspace of the zero total angular momentum $L = 0$, the energy spectrum of the exciton is derived, and the linear optical susceptibilities for the excitons with a heavy hole or a light hole are calculated, respectively. There exist significant differences of the excitonic properties between the nano-rings and quantum dots.

The nanoscopic semiconducting ring is described by an electron-hole pair $(i = e, h)$ with an effective band edge mass m_i^* moving in a x-y plane. The ring-like structure is well described by a double well potential,

$U\left(\vec{r}_i\right) = \frac{1}{2R_0^2} m_i^* \omega_i^2 \left(\vec{r}_i{}^2 - R_0^2\right)^2$, which reproduces a soft barrier $\frac{m_i^* \omega_i^2 R_0^2}{2}$ at the center of the sample produced by self-assembly [3,4]. Here, R_0 is the radius of the ring, ω_i is the characteristic frequency of the radial confinement, and a ring width $W \approx 2\sqrt{\frac{\hbar}{2m_i^* \omega_i}}$. The model Hamiltonian is thus given by:

$$\mathcal{H} = \sum_{i=e,h} \left[\frac{\vec{p}_i^2}{2m_i^*} + U\left(\vec{r}_i\right)\right] - \frac{e^2}{4\pi\varepsilon_0\varepsilon_r \left|\vec{r}_e - \vec{r}_h\right|}, \qquad (1)$$

where $\vec{r}_i = (x_i, y_i)$ and $\vec{p}_i = -i\hbar\vec{\nabla}_i$ denote the position vector and momentum operator, ε_0 is the vacuum permittivity, and ε_r is the static dielectric constant of the host semiconductor. It should be pointed out that the present *double-well* like confinement potential can be rewritten as $U\left(\vec{r}_i\right) = \frac{1}{2}m_i^* \omega_i^2 \left(r_i - R_0\right)^2 \frac{(r_i+R_0)^2}{R_0^2}$. If one replaces the operator r_i in factor $\frac{(r_i+R_0)^2}{R_0^2}$ by its mean value $\langle r_i \rangle = R_0$, the confinement potential returns to the widely used parabolic form [3,9,10]. On the other hand, in the limit of the small radius R_0 or for a small potential strength ω_i, the soft barrier at the ring center is very weak, and the description of the nano-ring is more close to that of a quantum dot (see Fig. 1). For a fixed ring width (or potential strength), the crossover from nano-rings to quantum dots is determined by $R_0 \sim \frac{\sqrt{2}}{2}W$ or $\frac{\hbar\omega_i}{2} \sim \frac{m_i^* \omega_i^2 R_0^2}{2}$, which means the lowest energy of radial confinement is comparable to the soft barrier at the ring center. It should also be pointed out that our double-well confinement potential has been used to calculate the far-infrared spectroscopy for a two-electron nano-ring [17], in good agreement with the recent experiment done by Lorke *et al.* [3].

Introducing the relative coordinate $\vec{r} = \vec{r}_e - \vec{r}_h$ and center-of-mass coordinate $\vec{R} = \frac{m_e^* \vec{r}_e + m_h^* \vec{r}_h}{m_e^* + m_h^*}$, the model Hamiltonian is divided into

$$H = \mathcal{H}_{cm}\left(\vec{R}\right) + \mathcal{H}_{rel}\left(\vec{r}\right) + \mathcal{H}_{mix}\left(\vec{R}, \vec{r}\right),$$

$$H_{cm} = \frac{\vec{P}_{cm}^2}{2M} + \frac{M\omega_{cm}^2}{2R_0^2}\left(\vec{R}^2 - R_0^2\right)^2,$$

$$H_{rel} = \frac{\vec{P}_{rel}^2}{2\mu} + \frac{\mu}{2}\frac{\left(m_h^{*3}\omega_e^2 + m_e^{*3}\omega_h^2\right)}{M^3 R_0^2}r^4 - \mu\omega_{rel}^2 r^2$$
$$\qquad - \frac{e^2}{4\pi\varepsilon_0\varepsilon_r r},$$

$$H_{mix} = -2\mu \left(\omega_e^2 - \omega_h^2\right) \left(\vec{\mathbf{R}} \cdot \vec{\mathbf{r}} - \frac{\vec{\mathbf{R}}^3 \cdot \vec{\mathbf{r}}}{R_0^2}\right)$$
$$+ \frac{\mu \omega_{rel}^2}{R_0^2}\left[R^2 r^2 + 2\left(\vec{\mathbf{R}} \cdot \vec{\mathbf{r}}\right)^2\right]$$
$$+ 2\mu \frac{\left(m_h^{*2}\omega_e^2 - m_e^{*2}\omega_h^2\right)}{M^2 R_0^2}\vec{\mathbf{R}} \cdot \vec{\mathbf{r}}^3, \qquad (2)$$

where $\mu = \frac{m_e^* m_h^*}{M}$ is the electron-hole reduced mass and $M = m_e^* + m_h^*$ is the total mass. We have also introduced a center-of-mass frequency $\omega_{cm} = \sqrt{\frac{(m_e^*\omega_e^2 + m_h^*\omega_h^2)}{M}}$ and a relative frequency $\omega_{rel} = \sqrt{\frac{m_h^*\omega_e^2 + m_e^*\omega_h^2}{M}}$. The main advantage of the separation of center-of-mass and relative coordinates is that the negative Coulomb interaction $-\frac{e^2}{4\pi\varepsilon_0\varepsilon_r r}$ appears in H_{rel} only, and the well-known poor-convergence of the parabolic basis is thus avoided when the characteristic scale of systems is beyond the effective Bohr radius [18].

We assume the wave function of the exciton in the form

$$\Psi = \sum_{\lambda,\lambda'} A_{\lambda,\lambda'} \psi_\lambda^{cm}\left(\vec{\mathbf{R}}\right) \psi_{\lambda'}^{rel}\left(\vec{\mathbf{r}}\right), \qquad (3)$$

where $\psi_\lambda^{cm}\left(\vec{\mathbf{R}}\right)$ and $\psi_{\lambda'}^{rel}\left(\vec{\mathbf{r}}\right)$ are the respective wave functions of the center-of-mass and the relative Hamiltonians H_{cm} and H_{rel}, which can be solved by the series expansion method introduced by Zhu *et al.* [19,20]. $\lambda = \{n_{cm}, m_{cm}\}$ and $\lambda' = \{n_{rel}, m_{rel}\}$ represent the quantum number pairs of the radial quantum number n and orbital angular momentum quantum number m. Due to the cylindrical symmetry of the problem, the total orbital angular momentum $L = m_{cm} + m_{rel}$ is a good quantum number of the exciton wave functions.

To obtain the coefficients $A_{\lambda,\lambda'}$, the total Hamiltonian is diagonalized in the space spanned by the product states $\psi_\lambda^{cm}\left(\vec{\mathbf{R}}\right)\psi_{\lambda'}^{rel}\left(\vec{\mathbf{r}}\right)$. First of all, we solve the single particle problem of center-of-mass and relative Hamiltonians H_{cm} and H_{rel}, keep several hundreds of the single particle states, and then pick up the low-lying energy levels to construct several thousands of product states. Note that our numerical diagonalization scheme is very efficient and essentially exact in the sense that the accuracy can be improved as required by increasing the total number of selected low-lying energy levels f. For instance, when the product states $f = 1024$ are kept in $L = 0$ subspace, the precision of the ground state energy has a relative convergence of $\sim 10^{-6}$.

Once the coefficients $A_{\lambda,\lambda'}$ are obtained, one can calculate directly the measurable properties, such as the linear optical susceptibility of the nano-rings, whose imaginary part is related to the absorption intensity measured by the near-infrared transmission. In theory, the linear optical susceptibility is proportional to the dipole matrix elements between one electron-hole pair j state and the vacuum state, which in turn is proportional to the os-

cillator strengths F_j. In the dipole approximation, it is given by [13,18,21]

$$F_j = \left|\int\int d\vec{\mathbf{R}} d\vec{\mathbf{r}} \Psi\left(\vec{\mathbf{R}}, \vec{\mathbf{r}}\right)\delta\left(\vec{\mathbf{r}}\right)\right|^2$$
$$= \left|\sum_{\lambda,\lambda'} A_{\lambda,\lambda'}\psi_{\lambda'}^{rel}\left(\mathbf{0}\right)\int d\vec{\mathbf{R}}\psi_\lambda^{cm}\left(\vec{\mathbf{R}}\right)\right|^2, \qquad (4)$$

where the factor $\psi_{\lambda'}^{rel}\left(\mathbf{0}\right)$ and the integral over $\vec{\mathbf{R}}$ ensure that only the excitons with $L = 0$ (or more precisely $m_{cm} = m_{rel} = 0$) are created by absorbing photons. Therefore, the frequency dependence of the linear optical susceptibility $\chi\left(\omega\right)$ can be expressed as [13,18,21]

$$\chi\left(\omega\right) \propto \sum_j F_j \cdot \left(\hbar\omega - E_g - E_j - i\Gamma\right)^{-1}, \qquad (5)$$

where E_g and E_j are the respective semiconducting band gap of InAs and the bound state energy levels of the exciton, and Γ has been introduced as a phenomenological broadening parameter.

In what follows we limit ourselves in the subspace $L = 0$. As an interesting example, we choose the parameters $m_e^* = 0.067m_e$ [3,9], the effective mass of the light hole $m_{lh}^* = 0.099m_e$, the effective mass of the heavy hole $m_{hh}^* = 0.335m_e$, and the appropriate parameter to InGaAs $\varepsilon_r = 12.4$. Moreover, the electron and hole are considered to be confined in the a confinement potential with the same strength, i.e., $m_e^*\omega_e^2 = m_h^*\omega_h^2$. If the characteristic energy and length scales are the effective Rydberg radius $R_y^* = \frac{\mu e^4}{2\hbar^2(4\pi\varepsilon_0\varepsilon_r)^2}$ and the effective Bohr radius $a_B^* = \frac{4\pi\varepsilon_0\varepsilon_r\hbar^2}{\mu e^2}$ for the heavy hole exciton, we find $R_y^* = 5.0$ meV and $a_B^* = 11.8$ nm. In order to simulate the InAs nano-rings with $\Delta E_m \sim 5$ meV and $\Delta E_n \sim 20 - 25$ meV in the experimental measurements [11], R_0 and $\hbar\omega_e$ are chosen to be 20 nm and 14 meV respectively ($\hbar\omega_e = 14$ meV corresponds to a ring width $W = 10$ nm). ΔE_m is the energy level spacing between the single electron states with different orbital angular momentum m and the same radial quantum number n, while ΔE_n corresponds to the energy spacing with different radial quantum number n and the same angular momentum m.

In Fig.2a and Fig.2b, the imaginary part of linear optical susceptibility with two different ring radii: $R_0 = 20$ nm and 5 nm is shown, where a broadening parameter $\Gamma = 2.5$ meV is used. The solid and dashed lines correspond to the heavy hole and light hole excitons. Those curves represent all the possible transitions of excitonic states which can be measured by photoluminescence excitation measurements (PLE). Comparing these two figures, one finds the following differences: i). For a large ring radius, only a few low-lying states transitions appear in the low photon energy regime. As photon energy increases, the intensity of transitions damps rapidly. ii). For a small ring radius, the low-lying states transitions

is nearly equally distributed in the whole photon energy regime both for the heavy-hole and light-hole excitons. iii). The intensity magnitude of the ground state transition in Fig.2b is almost one order smaller than that in Fig.2a. All these features amazingly coincide with the experimental observations between nano-rings and quantum dots structures [11]. Indeed, for the nano-ring with a smaller radius 5 nm, its width is comparable to the radius, $W \sim 2R_0$. The description of the small radius nano-ring should be equivalent to that of a quantum dot. The imaginary part of linear optical susceptibility for a cylindrical quantum dot in a parabolic potential $U(\vec{r}) = \frac{1}{2}m^*\omega_0^2 r^2$ ($\hbar\omega_0$ is taken to be 28 meV) is also displayed in Fig.2c, whose features are very similar to that of Fig.2b.

The distinct differences between nano-rings and quantum dots mainly originate from their geometries. For quantum dots, nearly periodic distributed low-energy transitions (the higher peaks in Figs. 2b or 2c) are reflections of electron-hole excitations involving the exciton ground state and various center-of-mass replicas without altering the ground state of the relative coordinate, while the smaller amplitude peaks of the photon energy at $1.341, 1.362, 1.368$ eV in Fig. 2b correspond to *internal* excited states of the exciton (its relative coordinate) [22]. However, for quasi-one-dimensional nano-rings, this situation is totally changed. The center-of-mass degrees of freedom are greatly suppressed by the anisotropic ring-like confinement and the relative motion becomes dominant, giving rise to the destruction of the regular patterns observed in quantum dots.

To fully understand the effects of ring radius R_0 on the optical properties, the transition peak's positions or the low lying energy levels of excitons and the corresponding oscillator strengths are plotted as a function of the ring radius in Fig.3a and Fig.3b, respectively. Each line is delineated by the transition sequence indicated in Fig.2b. The most striking feature is that the oscillator strengths F_j are approximately proportional to the ring radius. Amazingly, for $R_0 = 20$ nm, the oscillator strengths of the ground state and first excited transitions are nearly 30 and 10, in good agreement with the experimental values $F_j = 31$ and 18 [11]. Moreover, in Fig.3a and Fig.3b, the peak's positions show a few changes of the low lying transitions when $R_0 \geqslant 10$ nm.

Let us now compare the theoretical results with the near-infrared transmission data of H. Pettersson *et al.* [11]. In experiment, one cannot distinguish the contribution from the heavy hole or the light hole excitons. To reproduce the experimental result for an InAs nanoring, in Fig.4b we plot the combination of imaginary part of linear optical susceptibility of the heavy-hole and the light-hole excitons with the ring radius $R_0 = 20$ nm. Actual self-assembled nano-rings display a size distribution which greatly affects their physical features because each nano-ring is very small. To account for the experimental data, here a relatively large level broadening of $\Gamma = 5$ meV has been used. By fitting the rightmost peak's position in Fig. 4a, we take the band-gap E_g to be 1.325 eV. As shown in Fig.4, the overall trend of the experiment result is qualitatively reproduced by the model calculation, *i.e.*, both of them exhibit three transition peaks, and the peak's positions and relative amplitudes agree with each other *qualitatively*. The main discrepancy between the present theory and experiment occurs at high photon energy 1.4 eV, where the experimental curve displays a steep increase, while the theory predicts no variation. This discrepancy can be attributed to the increasing contribution from the wetting layer [23]. The small split of the rightmost peak is somewhat of a biasing artifact due to the unknown ratio of the contributions of the heavy hole and light hole excitons. However, considering the simplicity of our effective-mass model and the use of only one fitting parameter E_g, the overall fit is still quite surprising. Actually, more convincing fits should involve a suitable set of effective mass parameters, a careful adjusted confinenent strength, the realistic size distribution, the ratio of heavy hole and light hole excitons, and others unknown factors in experiments.

Recently, Warburton *et al.* presented a beautiful experiment of optical emission in a single charge-tunable nano-ring [4]. They studied the role of multiply-charged exciton complexes with no applied magnetic field and found a shell structure in energy similar to that of quantum dots [24,25]. Therefore, encouraged by the rapid developed nano-techniques for detection, i.e., the achievement of extremely narrow and temperature insensitive luminescence lines from a single InAs nano-ring in GaAs, we hope that our explanation of the distinct optical properties of quantum dots and nano-rings can be further confronted in a more precise experiment in the future.

In conclusion, we have studied the low lying exciton states and their optical properties in a self-assembled semiconducting InAs nano-ring. By varying the radius R_0, both the conventional quantum dots and nano-rings have been considered within the same framework of our theory. The distinct optical properties of quantum dots and nano-rings observed in recent experiments are well explained qualitatively.

[1] A. Lorke and R. J. Luyken, Physica B **256**, 424 (1998).

[2] A. Lorke, R. J. Luyken, M. Fricke, J. P. Kotthaus, G. Medeiros-Ribeiro, J. M. Garcia, and P. M. Petroff, Microelectronic Engineering **47**, 95 (1999).

[3] A. Lorke, R. J. Luyken, A. O. Govorov, J. P. Kotthaus,

J. M. Garcia, and P. M. Petroff, Phys. Rev. Lett. **84**, 2223 (2000).

[4] R. J. Warburton, C. Schäflein, D. Haft, F. Bickel, A. Lorke, K. Karrai, J. M. Garcia, W. Schoenfeld, and P. M. Petroff, Nature **405**, 926 (2000).

[5] T. Chakraborty and P. Pietiläinen, Phys. Rev. B **50**, 8460 (1994).

[6] V. Gudmundsson and Á. Loftsdóttir, Phys. Rev. B **50**, 17433 (1994).

[7] L. Wendler, V. M. Fomin, A. V. Chaplik, and A. O. Govorov, Phys. Rev. B **54**, 4794 (1996).

[8] V. Halonen, P. Pietiläinen, and T. Chakraborty, Europhys. Lett. **33**, 377 (1996).

[9] A. Emperador, M. Pi, M. Barranco, and A. Lorke, Phys. Rev. B **62**, 4573 (2000).

[10] H. Hu, J. -L. Zhu, and J. J. Xiong, eprint cond-mat/0005520, to be published in Phys. Rev. B (2000).

[11] H. Pettersson, R. J. Warburton, A. Lorke, K. Karrai, J. P. Kotthaus, J. M. Garcia, and P. M. Petroff, Physica E **6**, 510 (2000).

[12] I. Magnúsdóttir and V. Gudmundsson, Phys. Rev. B **60**, 16591 (2000).

[13] W. Que, Phys. Rev. B **45**, 11036 (1992).

[14] V. Halonen, T. Chakraborty and P. Pietiläinen, Phys. Rev. B **45**, 5980 (1992).

[15] A. Wojs and P. Hawrylak, Phys. Rev. B **51**,10880 (1995).

[16] P. Hawrylak, Phys. Rev. B **60**, 5597 (1999).

[17] H. Hu et al., unpublished.

[18] J. Song and S. E. Ulloa, Phys. Rev. B **52**, 9015 (1995).

[19] J. -L. Zhu, J. J. Xiong, and B. -L. Gu, Phys. Rev. B **41**, 6001 (1990).

[20] J. -L. Zhu, Z. Q. Li, J. Z. Yu, K. Ohno, and Y. Kawazoe, Phys. Rev. B **55**, 1 (1997).

[21] G. W. Bryant, Phys. Rev. B **37**, 8763 (1988).

[22] The smaller amplitude comes from the small oscillator strength of internal excited states, for example, due to the excitations of relative coordinate, the factor $\psi_{\lambda'}^{rel}(\mathbf{0})$ in Eq. 4 decreases and in turn lowers the oscillator strength.

[23] H. Pettersson, private communication.

[24] M. Bayer, O. Stern, P. Hawrylak, S. Fafard, and A. Forchel, Nature **405**, 923 (2000).

[25] P. Hawrylak, G. A. Narvaez, M. Bayer, and A. Forchel, Phys. Rev. Lett. **85**, 389 (2000).

Figures Captions

Fig.1. The confinement potential $U(\vec{\mathbf{r}}) = \frac{m_e^* \omega_e^2}{2R_0^2}\left(\vec{\mathbf{r}}^2 - R_0^2\right)^2$ with different ring radii with $m_e^* = 0.067 m_e$ and $\hbar\omega_e = 14$ meV.

Fig.2. Imaginary part of linear optical susceptibility for the nano-ring as a function of photon energy with two different ring radii $R_0 = 20$ nm (a) and $R_0 = 5$ nm (b). For comparison, the results for a parabolic quantum dot are also displayed (c). The solid and dashed lines correspond to the heavy-hole and light-hole excitons, respectively. The semiconducting band gap E_g is 1.325 eV.

Fig.3. The peak's positions of the linear optical susceptibility (a) and oscillator strengths (b) for the nano-ring as a function of the ring radius R_0. The square and solid circle symbols denote the heavy-hole and light-hole excitons, respectively. Each line is labeled by the sequence indicated in Fig.2(b).

Fig.4. The spectrum of the linear optical susceptibility of the nano-ring as a function of photon energy. (a) is the experimental result and (b) is our theoretical one.

Fig. 1

Low energy exction states in......
H. Hu *et al*.
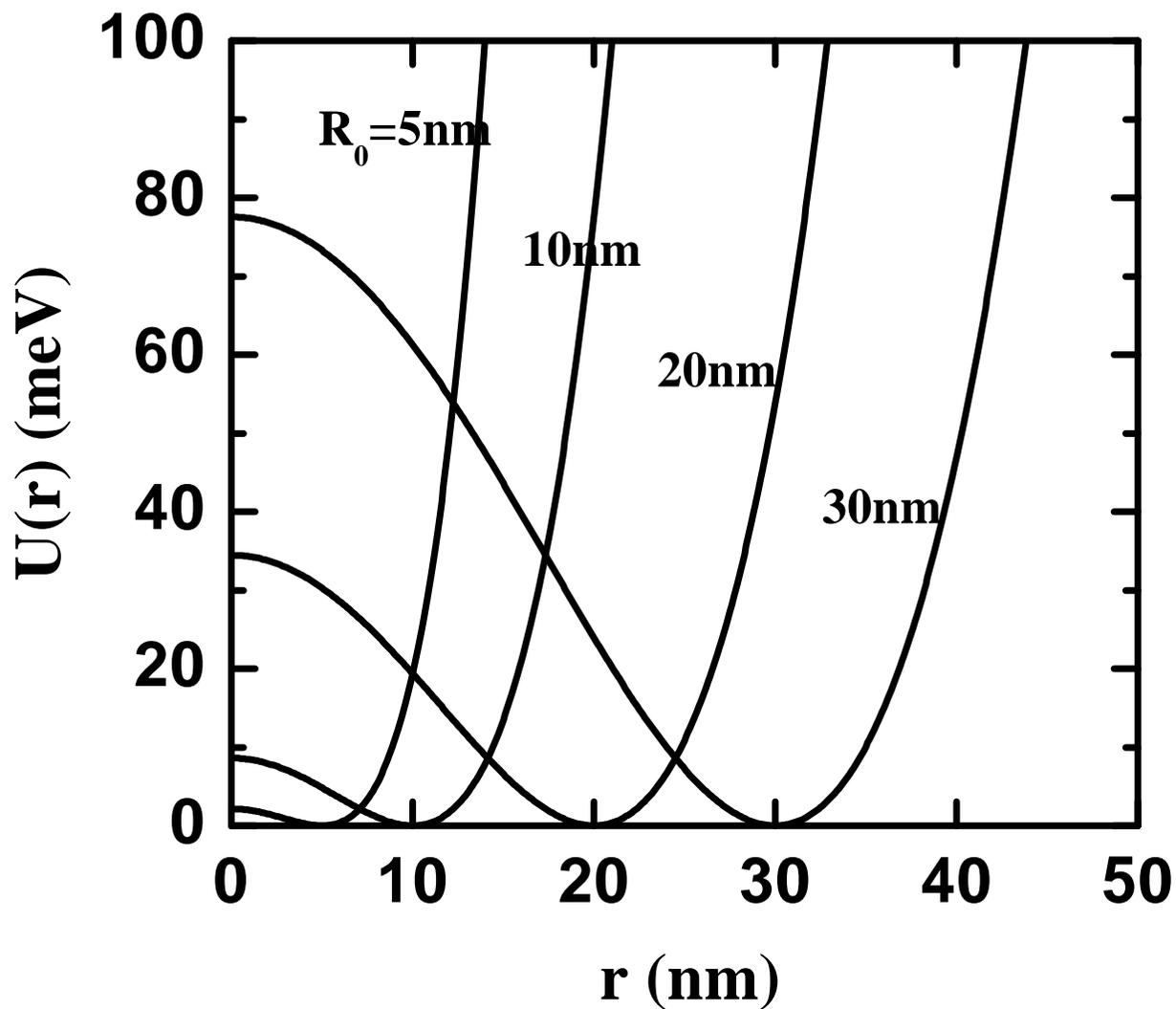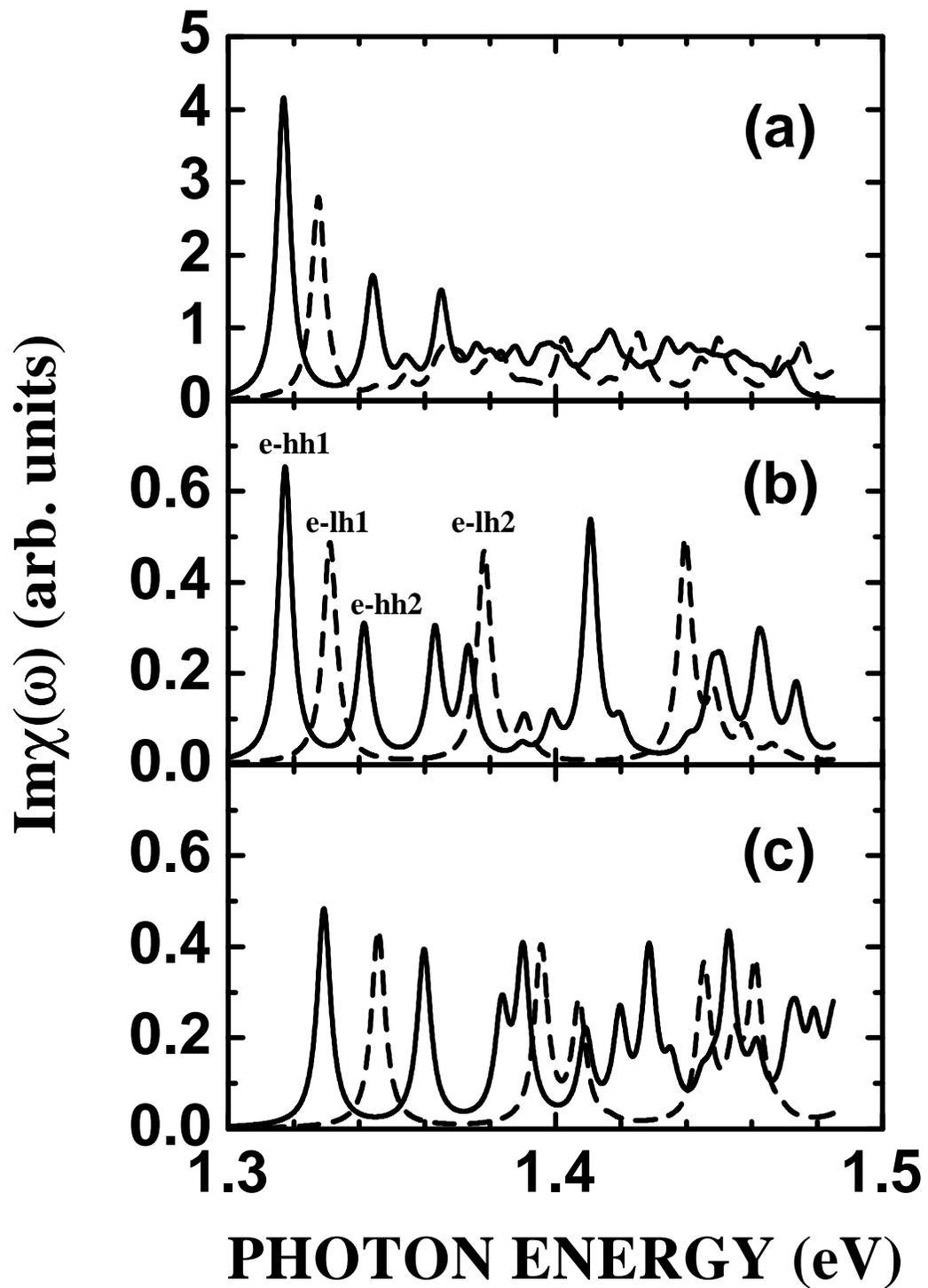
Fig. 2
Low energy exciton states in.....
H. Hu *et al.*

Fig. 2
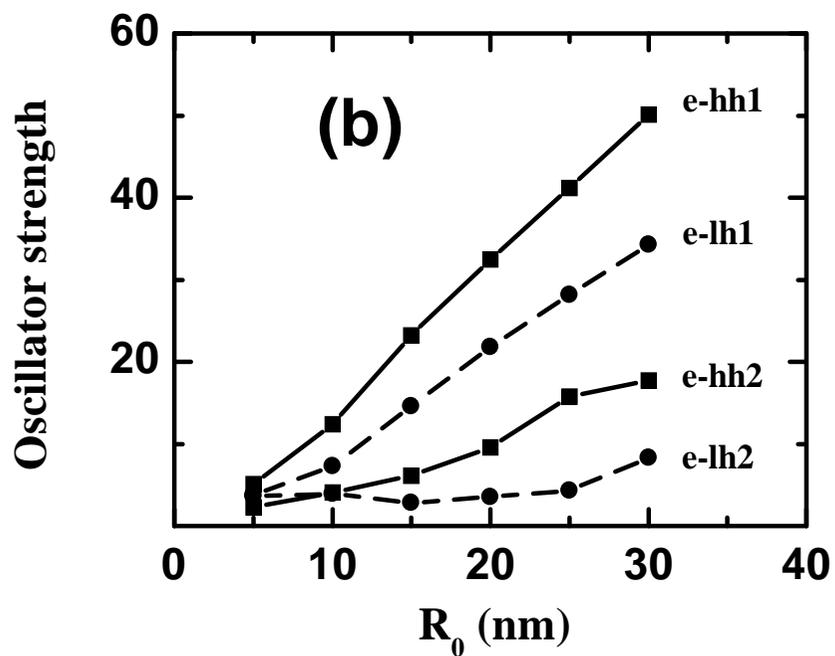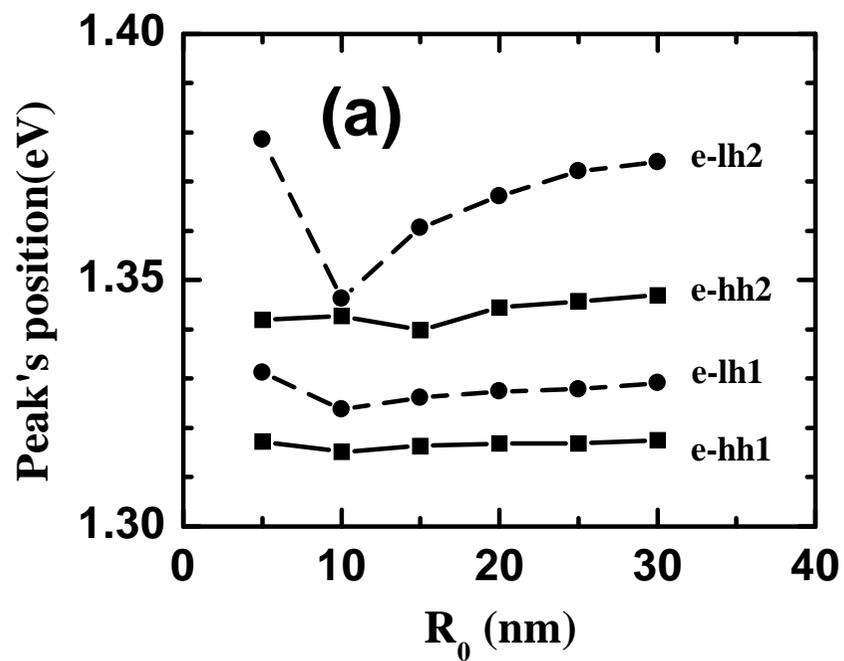
Fig. 3
Low energy exciton states in.....
H. Hu *et al.*

Fig. 3

Fig. 4